

Comparative study on doping of polyaniline with graphene and multi-walled carbon nanotubes

Elsayed M. Elnaggar¹ · Khalid I. Kabel² · Ahmed A. Farag² · Abdalrhman G. Al-Gamal²

Received: 5 September 2016 / Accepted: 6 January 2017 / Published online: 3 February 2017
© The Author(s) 2017. This article is published with open access at Springerlink.com

Abstract This study reported the doping of polyaniline (PANI) with graphene (G) and multi-walled carbon nanotubes (MWCNTs) by in situ polymerization. The molecular structure of PANI and its composites was observed by FTIR, which shows that the intensity of composites peaks are higher than pure PANI due to charge transfer between the PANI and graphitic allotropes. The structural information and crystallinity of PANI and its composites can be deduced from X-ray diffraction. The morphological characterization was observed by transmission electron microscope, which elucidated that aniline molecules were physically adsorbed and polymerized on the surface of graphene and MWCNTs due to π – π^* electron interaction. PANI represents as an external layer of composites with several diameters depending on the PANI deposition degree, where the cores are G and MWCNTs. The conductivity measurement clarified the conductivity value of 0.1 wt% G in PANI matrix is higher 17 times than PANI without it.

Keywords PANI/MWCNTs composites · PANI/graphene composites · Polyaniline composites

Introduction

Since the discovery of conductive polyacetylene (PA) by iodine doping [1], other π -conjugated polymers such as polypyrrole (PPy), polyaniline (PANI) and polythiophenes

(PTH) have been reported as conducting polymers (CPs) [2]. CPs are organic conjugated polymers which generally are comprised simply of C, H and simple heteroatoms such as N and S, where electrical properties are created by delocalizing the electrons of π -bond on conjugated chains of polymer [3]. Many advantages of CPs like as electrical conductivity, reversible electrochemical behavior, electrical and optical properties paid researchers for using it in several applications; as diverse as sensors [1, 2], polymer based energy storage devices [4, 5], plastic solar cells, or corrosion protection [6]. PANI nanostructure and its composites are widely studied, because its advantages are higher than other conductive polymers, represented by easy chemical and electrochemical polymerization [7–9], easy doping and de-doping by treatment with aqueous acid or base [10], and high resistance to environmental degradation. Zarras et al. reported that the electrical conductivity of PANI has a dramatic effect by doping and un-doping processes [11].

On the other hand, carbon allotropes including fullerene, single/multiwall carbon nanotubes (CNTs), graphite, diamond and graphene have attracted considerable attention over the last two decades because of their excellent properties and wide applications [12].

Among these allotropes, graphene (G) and MWCNTs, G sheet is a plan of monolayer carbon atoms arranged in non-spatial configuration two-dimensional (2D) honeycomb lattice with C–C bond length of 0.142 nm [13], while MWCNTs are considered as a series of single-walled carbon nanotubes, i.e., graphene sheets rolled into seamless cylinders, arranged coaxially with regular increase in the diameter [14]. Discovery of two promising carbon allotropes in 1991 and 2004, respectively, opened new advancement paths because of their unique properties, such as chemical and thermal stability, electronic properties,

✉ Elsayed M. Elnaggar
elsayed_elmhdy80@yahoo.com

¹ Department of Chemistry, Faculty of Science, Al-Azher University, Cairo, Egypt

² Department of Petroleum Applications, Egyptian Petroleum Research Institute, Nasr City, P.B. 11727, Cairo, Egypt



high tensile strength and ultra-light weight [15–21]. Those matchless properties paid researchers to use it in several scientific applications such as actuators, solar cells, field emission device, field effect transistor, super capacitors and batteries [22–25].

Doping PANI with G or MWCNTs was used in various target applications due to useful environmental stability, electrical, optical and reversible control of conductivity as well as superior mechanical strength compared to pure PANI. The combination of the PANI with graphitic allotropes is very attractive not only to reinforce conducting polymer but also to introduce new electronic properties based on the morphological modification or electronic interaction between the two components [26–29].

There are different ways to produce PANI/graphitic materials; one common method is in situ polymerization, it is used to produce composite with non-covalent bonds where the PANI matrix and graphitic filler interact through relatively weak dispersive forces which are represented by π – π infraction interaction between the quinoid rings of PANI and π -bond graphitic material lattice, calling physico-sorption [29–32].

PANI/G and PANI/MWCNT composites with different wt% ratios were synthesized by “in situ” polymerization. Properties of PANI and two composites were characterized by various analyses such as FTIR, XRD, TEM and Raman spectroscopy. Effects of doping PANI with G and MWCNTs on the electric conductivity of it were investigated by measuring electrical conductivity using standard two-probe technique.

Experimental

Materials

Commercial aniline, potassium peroxydisulfate (PPS), methanol and ethanol were purchased from El-Nasr Company for intermediate chemicals (NCIC) while hydrogen chloride (37%) and acetone were supplied from a Honeywell Company (USA). MWCNT was supplied from Egyptian Petroleum Institute (EPRI) with diameter 10–40 nm, length 10–100 μ m and number of walls nearly 40–50. Roads of graphene were provided from VEB Elektrokohle Lichtenberg, REKIPRO (Germany) and were crushed using Retsch ball mill PM400 (Germany).

Purification of aniline monomer

Aniline monomer (100 ml) was replaced in 250-ml round-bottomed glass flask, equipped with a condenser. The system is refluxed on a hot plate at 100 °C for 2 h to produce purified aniline (P-aniline).

Preparation of nano-PANI by in situ polymerization

PANI was synthesized by template-free method. 10 mmol of the P-aniline was mixed with 10 mmol of HCl, as doping agent, in 160 ml of distilled water and the solution was stirred in ice at 0 °C bath for 1 h to form a homogeneous solution of aniline–HCl. In the next step, 60 ml of aqueous solution containing 5 mmol of the PPS was added dropwise into the solution and stirred at the temperature of 0–5 °C for 2 h. Polymerization process is observed by changing the color of the solution. Then the polymer solution was kept at 0 °C for 2 days to complete the polymerization process. At the end of polymerization, the produced polymer was filtered on a filter paper and washed with 1 M HCl, acetone, methanol and finally with distilled water to remove any impurities. The polymer product was dried in an oven at 50 °C for 2 h. The obtained fine green powder is PANI–emeraldine salt (PANI–ES).

Nano-PANI-composites preparation

The composites of acid-doped PANI with MWCNTs and G were synthesized via in situ chemical polymerization. In a typical procedure of PANI, 10 mmol of aniline monomer was mixed with 10 mmol of HCl in 160 ml of distilled water and the solution was stirred in an ice bath at 0 °C for 1 h; every composite core (MWCNTs and G) had been taken in different weights, 0.1, 0.5 and 1%, proportional to aniline monomer ratio. The weighted composite core was dissolved in 20 ml of 1.0 M HCl solution and sonicated over 2 h in an ultrasonic bath, then mixed with aniline–HCl solution by magnetic stirrer. Afterwards, 60 ml of aqueous solution containing 5 mmol of PPS was added dropwise into the suspension and the mixture was stirred at 0–5 °C for 2 h. Subsequently, the samples were kept at 0 °C to complete polymerization process. The products were filtrated and washed with HCl 1 M, acetone–methanol and finally with distilled water to remove any impurities and the products were dried at 50 °C for 2 h in a Petri dish to prevent aggregation of PANI nanoparticles. The synthesized composites are arranged according to PANI/composite ratios in Table 1.

Table 1 PANI/composites ratios

No.	Sample	Composite core (wt%)
1	PANI/P-MWCNT ₁	0.1
2	PANI/P-MWCNT ₂	0.5
3	PANI/P-MWCNT ₃	1.0
4	PANI/G ₁	0.1
5	PANI/G ₂	0.5
6	PANI/G ₃	1.0



Conductivity measurement of polyaniline and polyaniline composites

The electrical conductivity was obtained by measuring the resistance of synthesized composites PANI, PANI/MWCNTs_{1,2and3} and PANI/G_{1,2and3} at room temperature using two-probe method [33]. The synthesized composites were dried in a vacuum and pressed into a pellet, with diameter 1.10 cm and thickness 1.3 mm. Then the sample was placed between two electrodes and specified current was passed through it while the resistances were measured using digital multimeter (UNI-T; UT33C, Germany). The average value of the resistance of each composite was taken at five different points. The conductivity was calculated through resistance by applying the following equation:

$$\sigma (\text{S/cm}) = 1/R (\Omega) \times A (\text{cm}^2) \quad (1)$$

where σ is conductivity, R is resistance and A is the surface area.

Instrumentation

X-ray diffraction (XRD) analysis was performed on an X-ray diffractometer from PANalytical company model (X'Pert Pro) with 2θ from 10 to 90 and conditions 40 mA, 40 kV and wavelength of Copper $K\alpha_1$ at 1.54 Å. The Fourier transform infrared spectroscopy (FTIR) spectrum (400–4000 cm^{-1}) was measured. The addition of carboxyl and hydroxyl groups on the CNT surface using Thermo Fisher Scientific; Nicolet iS10 FTIR Spectrometer, USA; the sample was mixed with pure KBr as the background, then the mixture was dried and compressed into a transparent tablet for measurement. Raman laser was used at an excitation source wavelength of 532 nm, the Raman analysis was carried out using dispersive Raman spectroscopy, Senterra, Bruker, Germany. The laser spot size was 1 μm and the temperature of the sample was kept at room temperature. The thermal stability was assessed by thermal gravimetric analysis (TGA) (SDT Q600 V20.5 Build 15) in the temperature range of 20–850 °C (10 °C/min) under a nitrogen atmosphere. The shape and the surface morphology of the samples were analyzed using high-resolution transmission electron microscope (HRTEM) (JEOL-JEM-2100F, Japan) at 200 kV. The samples were sonicated by ultrasonic bath to disperse the aggregation (Sonic Star, 50 kHz, and 300 W).

Results and discussion

FTIR characterization

Molecular structure of PANI and its composite (PANI/MWCNTs and PANI/G) is supported by FTIR

spectroscopy and its data sheet is presented in Figs. 1 and 2, while Table 2 explains the characteristic frequencies of the PANI and PANI/composites. The spectrum of prepared PANI in an aqueous media shows several peaks, the main peaks are situated at 1559 cm^{-1} (with a shoulder at 1617 cm^{-1}), 1475, 1408, 1401, 1301, 1242, 1126, 803, 580 and 505 cm^{-1} . The peak at 580 cm^{-1} is attributed to vibration of the sulfate anions which ionized from the oxidizing agent (PPS) during the polymerization process; the ionized sulfate ions linked to nitrogen atoms in PANI by ionic bond which explains why PANI doped in part of it [31, 32, 34–37]. After coating graphitic materials (MWCNTs and G) with PANI, the spectra reflect the presence of polymer overlay. The interaction between graphitic materials (MWCNTs and G) and CPs manifested by PANI peaks shifts and intensity increases [31, 32, 38–40], the spectrum is approximately similar to PANI spectrum, however, exhibits changes in the intensity of the bands at about 1242 cm^{-1} and the prominent band at 1121 cm^{-1} differed slightly in shape and shifted to higher wave number [32, 34, 41]. These changes interpret the

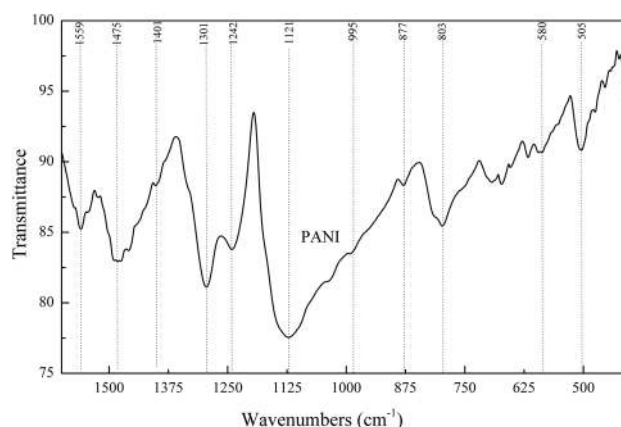


Fig. 1 FTIR spectra of PANI

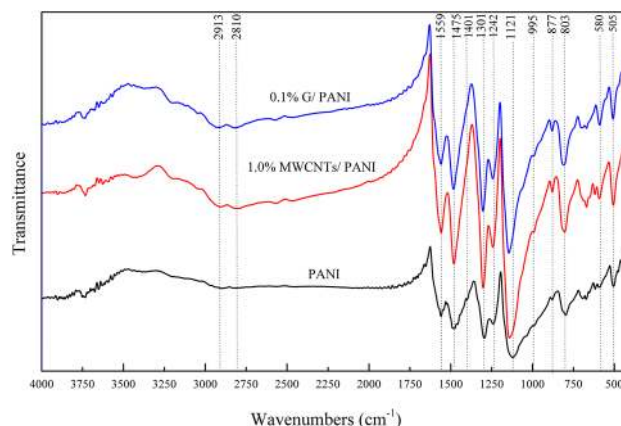
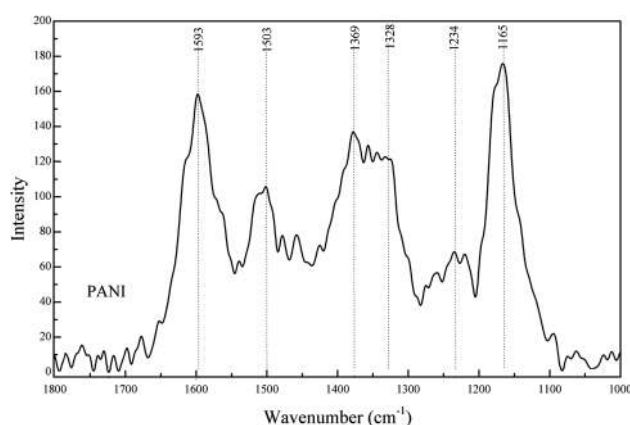


Fig. 2 FTIR spectra of PANI/graphitic allotropes (MWCNTs and G)



Table 2 FTIR characteristic frequencies of PANI and PANI/composites

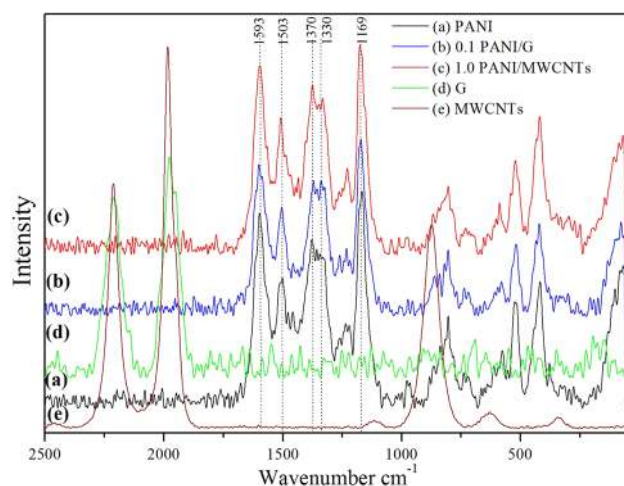
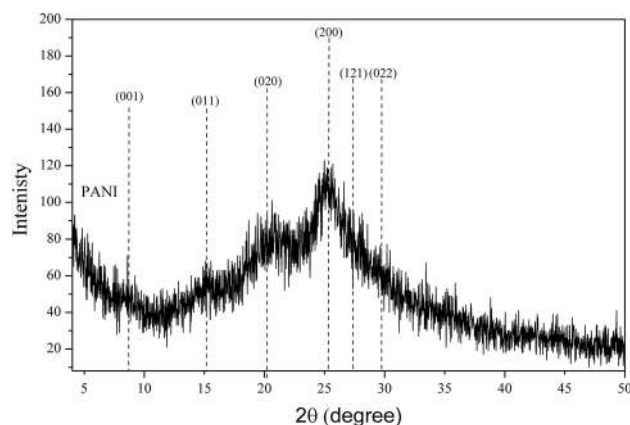
Wavenumber (cm^{-1})	Band characteristics	References
1559	C=N stretching deformation of the quinoid ring	[31, 32]
1475	C=C stretching deformation of benzenoid rings	[32, 34]
1401	C-N ⁺ hydrogen-bonded vibration	[40]
1301	C-N stretching of secondary aromatic amine	
1242	C-N ⁺ stretching and vibration in the polaron structure of PANI	[40]
1121	The aromatic C-H in-plane bending	
995	C-Cl group vibration	[34]
877	C-H bond out-of-plane deformation, vibration of 1,2,4-disubstituted benzene	[34]
803	C-H deformation out-of-plane of the 1,4-disubstituted benzene ring	[31, 32, 34]
580	Stretching vibration in the sulfate anion	[32, 34]
505	C-H deformation out-of-plane of the 1,4-disubstituted benzene ring	[31]
2810	Methylene groups stretching present in MWCNTs and G	
2913	Methylene groups stretching present in MWCNTs and G	

**Fig. 3** Raman spectra of PANI

charge transfer between the PANI and graphitic materials (MWCNTs and G), hence improving the electrical conductivity of PANI.

Raman analysis

Raman spectroscopy is a very useful technique for characterizing the material composition [48]. Nano-PANI and its composites (PANI/MWCNTs and PANI/G) were observed. Figure 3 shows the Raman spectra of PANI; the C-H bending of the quinoid ring ($-N=Q=N-$) at 1165 cm^{-1} , C-H bending of the benzenoid ring ($-N=B=N-$) at 1235 cm^{-1} , C-N⁺ stretching at 1328 cm^{-1} with (shoulder extending to higher wave number at 1370 cm^{-1}), and C-C stretching of the benzene ring at 1503 and 1593 cm^{-1} were observed proving the presence of the doped PANI structures [31, 42]. The spectrum of graphitic materials and PANI/composites in Fig. 4 shows

**Fig. 4** Raman spectra of graphitic material PANI/graphitic allotropes composites**Fig. 5** XRD spectrum of PANI

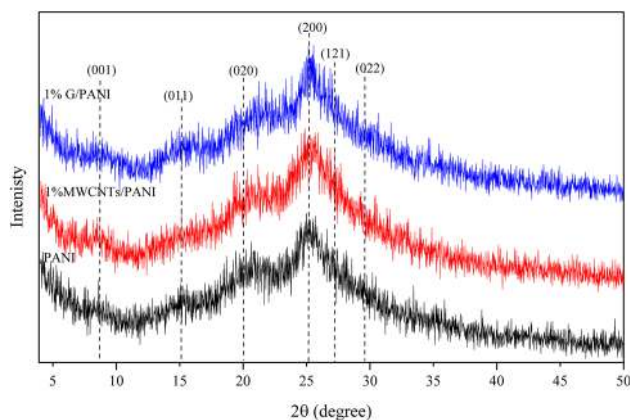


Fig. 6 XRD analysis of PANI/graphitic allotropes (MWCNTs and G)

that PANI is dominant in all composites with various ratios. This result confirms the good covering of composites with PANI. By careful inspection of Fig. 4, it can be observed that all band positions were shifted to higher wave numbers and the intensity of the peaks at 1328 and 1593 cm^{-1} was increased because they are very close to

the D and G modes of graphitic materials, which interprets a strong interaction between graphitic allotropes and PANI due to π - π^* electron interaction between MWCNTs or G and PANI [42].

XRD analysis

The structural information and crystallinity of PANI and its composite can be deduced from XRD of the samples. Figure 5 shows typical XRD patterns of PANI specimens, the crystalline peaks appeared at $2\theta = 9.1, 15.2, 20.3, 25.3, 27.4$ and 29.88 corresponding to (001), (011), (020), (200), (121) and (022) crystallographic planes reflections of PANI in its emeraldine salt (PANI-ES) [26, 29] indicating the efficient formation of conductive nano-PANI. XRD patterns of MWCNTs/PANI and G/PANI composites (Fig. 6) are quite similar to the pattern of PANI, the diffraction peaks of PANI can only be observed [29, 43] as seen in Fig. 7. XRD spectrum indicating no additional crystalline order had been introduced to the PANI. The intensity of (200) reflection was enhanced by increasing the

Fig. 7 TEM images of PANI. **a** Powders containing a small portion of nanofibers, **b** polymerization at initiation stage, **c** at propagation stage and **d** at termination stage

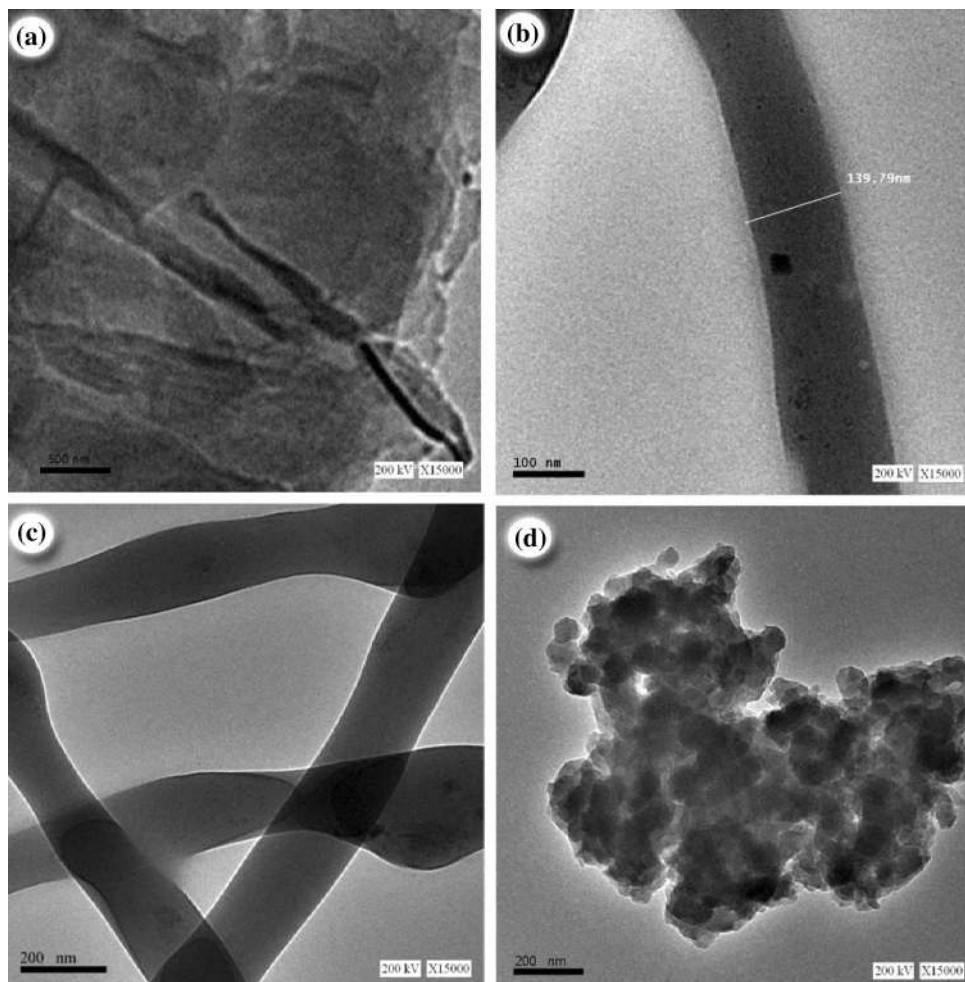
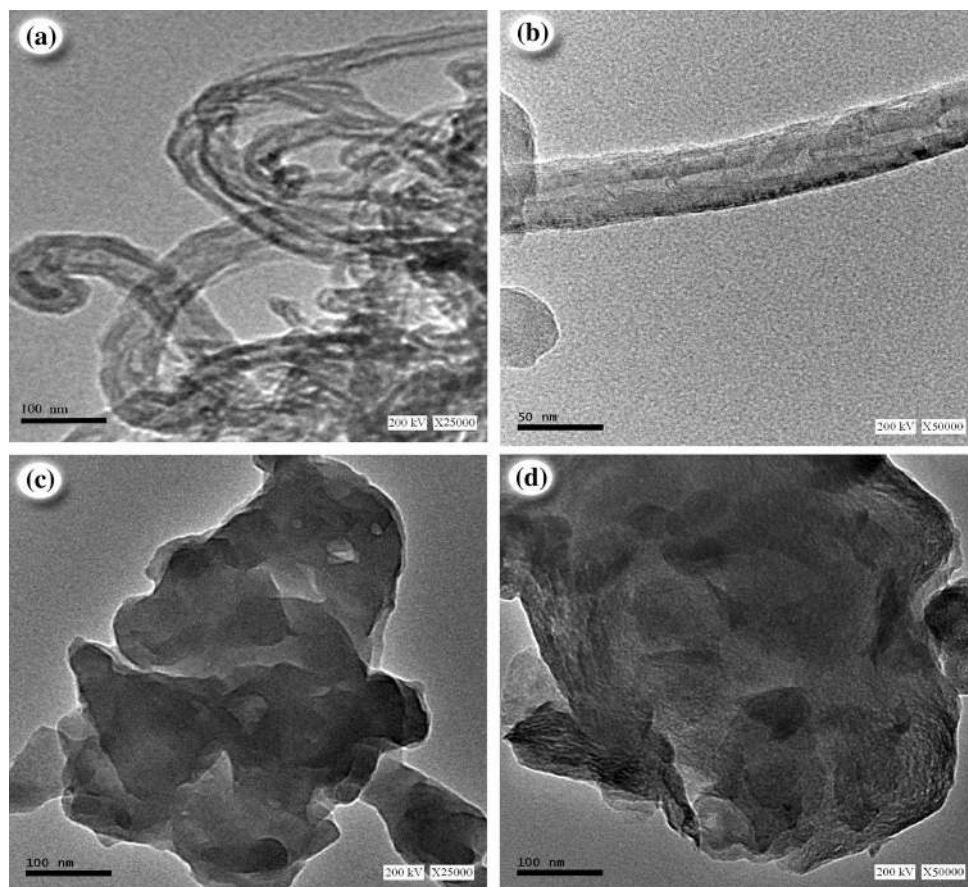


Fig. 8 TEM characterization of PANI/graphitic material. **a**, **b** TEM images of PANI/P-MWCNTs composite with different magnifications and **c**, **d** TEM images of PANI/G composite with different magnifications



ratio wt% of composites (MWCNTs and G); it is possibly due to overlapping the main peaks of PANI and graphitic materials.

Morphological characterization

HRTEM was used to observe morphology, nanoparticle size, measurement of grain size, crystallite size, the growth of layers, composition defects and atomic arrangement in prepared materials (PANI, PANI/MWCNTs and PANI/G). The observed images of PANI, PANI/P-MWCNTs and PANI/G are presented in Figs. 7 and 8. PANI nanostructures such as nanofibers, nanowires, nanorods, and nanotubes can be introduced and controlled in its morphology “structural directors” through the chemical polymerization method. In this work, PANI was synthesized by traditional oxidative in situ chemical polymerization, the traditional oxidative in situ chemical polymerization route is known to yield granular particles [3, 44, 45]. By carefully examining the morphology of PANI powders (Fig. 7a), it can be found that there is also a small portion of nanofibers agglomerated with granular particles [46].

We characterized PANI morphology at different polymerization stages, small amounts of product periodically

were extracted from the reaction bath at various times and then diluted with distilled water and observed by TEM. When polymerization started, initiation stage, nanofibers of PANI were formed [46], with average diameters of 130–145 nm, clearly seen in Fig. 7b. The propagation stage began when more PPS shared into the reaction, the nanofibers of PANI chains intertwined with each other and secondary morphology of PANI become such as scaffolds see Fig. 7c. Finally, in the termination stage, PANI turns into irregular agglomerate shape, containing nanofibers and granular particulates (Fig. 7d); therefore, it is surprising to know that some nanofibers can escape and remain in the final product [46, 47]. TEM images of PANI/MWCNTs in Fig. 8a, b showed uniform deposition of PANI on the surface of P-MWCNTs which manifested from the bilayered structure; the external layer is PANI with diameter ≈ 55 nm and the internal is CNT with diameter 10–40 nm, as the internal cavity is well discernible. Coating of MWCNTs with PANI takes place only on the outer surface of the MWCNTs where the polymerization of aniline inside the tubes of the CNTs is hindered and restricted by van der Waals force between tubes [31]. TEM images of PANI/G composite (Fig. 8c, d) show a black layer of G with enormous wavy shape wrinkled on its surface [48],



Table 3 The resistivity and electrical conductivity values of PANI and PANI/composites

Sample	σ (S/cm)
PANI-ES	6.9×10^{-3}
PANI/P-MWCNT ₁	1.2×10^{-2}
PANI/P-MWCNT ₂	2.0×10^{-2}
PANI/P-MWCNT ₃	4.0×10^{-2}
PANI/G ₁	1.2×10^{-1}
PANI/G ₂	5.8×10^{-2}
PANI/G ₃	2.4×10^{-2}

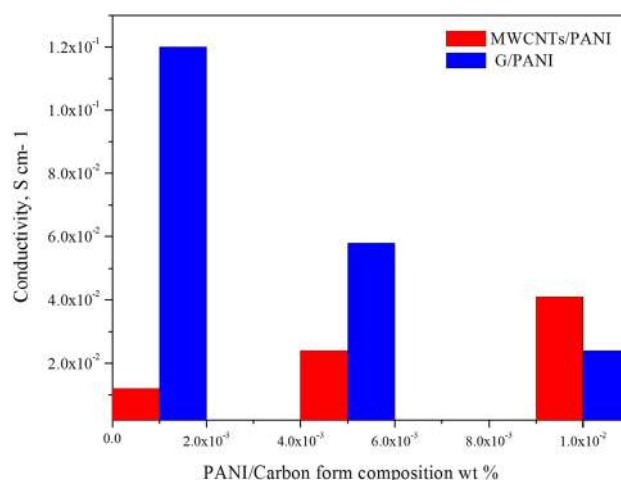
these wrinkles interpreted physical adsorption of PANI nanoparticles on graphene sheet's surface due to π - π interaction force that was explicated by Raman analysis. The various weight ratios of graphitic materials had no effect on the morphological characteristics of PANI/P-MWCNTs and PANI/G composites because P-MWCNTs or G ratio was very small relative to PANI.

Conductivity measurement of synthesized composites

The conductivity of PANI and its composites MWCNTs/PANI and G/PANI with various ratios was measured according to two-probe method [33]. The resistivity and electrical conductivity of synthesized materials are shown in Table 3. The listed results clarified that the electrical conductivity value of MWCNTs/PANI composite is rising with MWCNTs ratio increasing from 0.1 to 1%, this may be because MWCNTs serve as a “conducting bridge” between the PANI-ES conducting domains leading to enhance the electrical conductivity of PANI nanoparticles [49]. In spite of the higher electrical conductivity of PANI/G composite as compared to PANI where G may serve as a dopant of PANI [29], conductivity was reduced with G ratio increase. Graphene would be partially oxidized by PPS to graphene oxide (GO) sheets [50]. GO plates are electrically insulating material because of the disruption in their conjunction system [51], so these oxidized layers may act as insulating area between PANI-ES conducting domains and lead to diminish the conductivity value of PANI/G composite when G ratio increases. By careful examination of results (Fig. 9), we can observe that the conductivity of PANI/G composites is higher than counterpart PANI/MWCNTs composites because the surface area of graphene sheets is higher than CNTs.

Conclusion

In this work, PANI/G and PANI/MCWNT composites were prepared via the in situ polymerization. FTIR, Raman and XRD spectroscopy prove that two allotropic

**Fig. 9** Conductivity diagram of PANI/graphitic isotopes composites with various wt% ratios

composites take the same behavior, but they differ in morphological characterization and conductivity measurements. PANI/G composite takes plate shape while the shape of PANI/MCWNT composite is tubular, thus proving that PANI formed according to graphitic allotrope format. The conductivity measurements indicate the behavior of PANI/G is in contrast to PANI/MCWNT due to the difference between graphitic allotropes and polymerization oxidizing agent in shape and sensitivity.

Acknowledgements The authors acknowledge both Chemistry Department, Faculty of Science, Al-Azhar University and the Egyptian Petroleum Research Institute (EPRI), Cairo, Egypt, for the financial assistance and facilitation of our study.

Open Access This article is distributed under the terms of the Creative Commons Attribution 4.0 International License (<http://creativecommons.org/licenses/by/4.0/>), which permits unrestricted use, distribution, and reproduction in any medium, provided you give appropriate credit to the original author(s) and the source, provide a link to the Creative Commons license, and indicate if changes were made.

References

- Shirakawa, H., Louis, E. J., MacDiarmid, A.G., Chiang, C.K., Heeger, A.J.: Synthesis of electrically conducting organic polymers: halogen derivatives of polyacetylene, (CH)_x. J. Chem. Soc. Chem. Commun. 578–580 (1977). doi:10.1039/c39770000578
- Nalwa, H.S.: Encyclopedia of Nanoscience and Nanotechnology. CRC Press, Boca Raton (2004)
- Chandrasekhar, P.: Conducting Polymers, Fundamentals and Applications: A Practical Approach. Springer, Berlin (2013)
- Chiang, J.C., MacDiarmid, A.G.: ‘Polyaniline’: protonic acid doping of the emeraldine form to the metallic regime. Synth. Met. 13, 193–205 (1986)
- MacDiarmid, A.G., Epstein, A.J.: Polyanilines: a novel class of conducting polymers. Faraday Discuss. Chem. Soc. 88, 317–332 (1989)



6. Mostafaei, A., Nasirpour, F.: Epoxy/polyaniline–ZnO nanorods hybrid nanocomposite coatings: synthesis, characterization and corrosion protection performance of conducting paints. *Prog. Org. Coat.* **77**, 146–159 (2014)
7. Prasad, G., Takei, T., Yonesaki, Y., Kumada, N., Kinomura, N.: Hybrid nanocomposite based on NbWO₆ nanosheets and polyaniline. *Mater. Lett.* **60**, 3727–3730 (2006)
8. Sharma, B.K., Gupta, A.K., Khare, N., Dhawan, S., Gupta, H.: Synthesis and characterization of polyaniline–ZnO composite and its dielectric behavior. *Synth. Met.* **159**, 391–395 (2009)
9. Patil, R., Radhakrishnan, S.: Conducting polymer based hybrid nano-composites for enhanced corrosion protective coatings. *Prog. Org. Coat.* **57**, 332–336 (2006)
10. Slonczewski, J., Weiss, P.: Band structure of graphite. *Phys. Rev.* **109**, 272–279 (1958)
11. Zarras, P., Anderson, N., Webber, C., Irvin, D., Irvin, J., Guenther, A., Stenger-Smith, J.: Progress in using conductive polymers as corrosion-inhibiting coatings. *Radiat. Phys. Chem.* **68**, 387–394 (2003)
12. Anderson, M.R., Mattes, B.R., Reiss, H., Kaner, R.B.: Conjugated polymer films for gas separations. *Science* **252**, 1412–1415 (1991)
13. Yu, D., Dai, L.: Self-assembled graphene/carbon nanotube hybrid films for supercapacitors. *J. Phys. Chem. Lett.* **1**, 467–470 (2009)
14. Bhushan, B.: *Springer Handbook of Nanotechnology*. Springer, Berlin (2010)
15. Klumpp, C., Kostarelos, K., Prato, M., Bianco, A.: Functionalized carbon nanotubes as emerging nanovectors for the delivery of therapeutics. *Biochem. Biophys. Acta* **1758**, 404–412 (2006)
16. Zhao, L., Liu, H., Hu, N.: Electroactive films of heme protein-coated multiwalled carbon nanotubes. *J. Colloid Interface Sci.* **296**, 204–211 (2006)
17. Mu, Q., Liu, W., Xing, Y., Zhou, H., Li, Z., Zhang, Y., Ji, L., Wang, F., Si, Z., Zhang, B.: Protein binding by functionalized multiwalled carbon nanotubes is governed by the surface chemistry of both parties and the nanotube diameter. *J. Phys. Chem. C* **11**, 3300–3307 (2008)
18. Kathi, J., Rhee, K.: Surface modification of multi-walled carbon nanotubes using 3-aminopropyltriethoxysilane. *J. Mater. Sci.* **43**, 33–37 (2008)
19. Stoner, B., Brown, B., Glass, J.: Selected topics on the synthesis, properties and applications of multiwalled carbon nanotubes. *Diam. Relat. Mater.* **42**, 49–57 (2014)
20. Novoselov, K.S., Geim, A.K., Morozov, S., Jiang, D., Zhang, Y., Dubonos, S.A., Grigorieva, I., Firsov, A.: Electric field effect in atomically thin carbon films. *Science* **306**, 666–669 (2004)
21. Novoselov, K., Jiang, D., Schedin, F., Booth, T., Khotkevich, V., Morozov, S., Geim, A.: Two-dimensional atomic crystals. *Proc. Nat. Acad. Sci. USA* **102**, 10451–10453 (2005)
22. Popov, V.N.: Carbon nanotubes: properties and application. *Mater. Sci. Eng. R* **43**, 61–102 (2004)
23. Thostenson, E.T., Ren, Z., Chou, T.W.: Advances in the science and technology of carbon nanotubes and their composites: a review. *Compos. Sci. Technol.* **61**, 1899–1912 (2001)
24. Li, C., Thostenson, E.T., Chou, T.W.: Sensors and actuators based on carbon nanotubes and their composites: a review. *Compos. Sci. Technol.* **68**, 1227–1249 (2008)
25. Li, C., Li, Z., Zhu, H., Wang, K., Wei, J., Li, X., Sun, P., Zhang, H., Wu, D.: Graphene nano-“patches” on a carbon nanotube network for highly transparent/conductive thin film applications. *J. Phys. Chem. C* **114**, 14008–14012 (2010)
26. Wu, T.M., Lin, Y.W.: Doped polyaniline/multi-walled carbon nanotube composites: preparation, characterization and properties. *Polymer* **47**, 3576–3582 (2006)
27. Lafuente, E., Callejas, M.A., Sainz, R., Benito, A.M., Maser, W.K., Sanjuán, M., Saurel, D., Teresa, J., Martinez, M.T.: The influence of single-walled carbon nanotube functionalization on the electronic properties of their polyaniline composites. *Carbon* **46**, 1909–1917 (2008)
28. Gao, Z., Wang, F., Chang, J., Wu, D., Wang, X., Wang, X., Xu, F., Gao, S., Jiang, K.: Chemically grafted graphene-polyaniline composite for application in supercapacitor. *Electrochim. Acta* **133**, 325–334 (2014)
29. Papathanassiou, A.N., Mykhailiv, O., Echegoyen, L., Sakellis, I., Plonska, M.E.: Electric properties of carbon nano-onion/polyaniline composites: a combined electric modulus and ac conductivity study. *J. Phys. D Appl. Phys.* **49**, 285305 (2016)
30. Papathanassiou, A.N., Plonska, M.E., Mykhailiv, O., Echegoyen, L., Sakellis, I.: Combined high permittivity and high electrical conductivity of carbon nano-onion/polyaniline composites. *Synth. Met.* **209**, 583–587 (2015)
31. Konyushenko, E.N., Stejskal, J., Trchová, M., Hradil, J., Kovářová, J., Prokeš, J., Cieslar, M., Hwang, J.-Y., Chen, K.-H., Sapurina, I.: Multi-wall carbon nanotubes coated with polyaniline. *Polymer* **47**, 5715–5723 (2006)
32. Wu, Z., Chen, X., Zhu, S., Zhou, Z., Yao, Y., Quan, W., Liu, B.: Enhanced sensitivity of ammonia sensor using graphene/polyaniline nanocomposite. *Sens. Actuator B: Chem.* **178**, 485–493 (2013)
33. Devi, D.P., Bipinbal, P., Jabin, T., Kutty, S.K.: Enhanced electrical conductivity of polypyrrole/polypyrrole coated short nylon fiber/natural rubber composites prepared by in situ polymerization in latex. *Mater. Des.* **43**, 337–347 (2013)
34. Wan, M.: *Conducting Polymers with Micro or Nanometer Structure*. Springer, Berlin (2008)
35. Murugan, A.V., Muraliganth, T., Manthiram, A.: Rapid facile microwave-solvothermal synthesis of graphene nanosheets and their polyaniline nanocomposites for energy storage. *Chem. Mater.* **21**, 5004–5006 (2009)
36. Holly, S., Sohár, P.: Absorption spectra in the infrared region: a theoretical and technical introduction. *Akadémi Kiadó, Budapest* (1975)
37. Quillard, S., Louam, G., Buisson, J., Boyer, M., Lapkowski, M., Pron, A., Lefrant, S.: Vibrational spectroscopic studies of the isotope effects in polyaniline. *Synth. Met.* **84**, 805–806 (1997)
38. Deng, M., Yang, B., Hu, Y.: Polyaniline deposition to enhance the specific capacitance of carbon nanotubes for supercapacitors. *J. Mater. Sci.* **40**, 5021–5023 (2005)
39. Yu, Y., Che, B., Si, Z., Li, L., Chen, W., Xue, G.: Carbon nanotube/polyaniline core-shell nanowires prepared by in situ inverse microemulsion. *Synth. Met.* **150**, 271–277 (2005)
40. Yu, Y., Ouyang, C., Gao, Y., Si, Z., Chen, W., Wang, Z., Xue, G.: Synthesis and characterization of carbon nanotube/polypyrrole core-shell nanocomposites via in situ inverse microemulsion. *J. Polym. Sci. Part A Polym. Chem.* **43**, 6105–6115 (2005)
41. Liu, N., Luo, F., Wu, H., Liu, Y., Zhang, C., Chen, J.: One-step ionic-liquid-assisted electrochemical synthesis of ionic-liquid-functionalized graphene sheets directly from graphite. *Adv. Funct. Mater.* **18**, 1518–1525 (2008)
42. Farbod, M., Tadavani, S.K.: Electrical properties and glass transition temperature of multi walled carbon nanotube/polyaniline composites. *J. Noncryst. Solids* **358**, 1339–1344 (2012)
43. Hu, F., Li, W., Zhang, J., Meng, W.: Effect of graphene oxide as a dopant on the electrochemical performance of graphene oxide/polyaniline composite. *J. Mater. Sci. Technol.* **30**, 321–327 (2014)
44. Skotheim, T.A.: *Handbook of Conducting Polymers*. CRC Press, Boca Raton (1997)
45. Avlyanov, J.K., Josefowicz, J.Y., MacDiarmid, A.G.: Atomic force microscopy surface morphology studies of ‘in situ’ deposited polyaniline thin films. *Synth. Met.* **73**, 205–208 (1995)
46. Huang, J., Kaner, R.B.: A general chemical route to polyaniline nanofibers. *J. Am. Chem. Soc.* **126**, 851–855 (2004)



47. Huang, J., Kaner, R.B.: Nanofiber formation in the chemical polymerization of aniline: a mechanistic study. *Angew. Chem.* **116**, 5941–5945 (2004)
48. Li, R., Liu, L., Yang, F.: Preparation of polyaniline/reduced graphene oxide nanocomposite and its application in adsorption of aqueous Hg(II). *Chem. Eng. J.* **229**, 460–468 (2013)
49. Wu, T.M., Lin, Y.W., Liao, C.S.: Preparation and characterization of polyaniline/multi-walled carbon nanotube composites. *Carbon* **43**, 734–740 (2005)
50. Posudievsky, O.Y., Khazieieva, O.A., Koshechko, V.G., Pokhodenko, V.D.: Preparation of graphene oxide by solvent-free mechanochemical oxidation of graphite. *J. Mater. Chem.* **22**, 12465–12467 (2012)
51. Dreyer, D.R., Park, S., Bielawski, C.W., Ruoff, R.S.: The chemistry of graphene oxide. *Chem. Soc. Rev.* **39**, 228–240 (2010)

